




# An Aeropendulum-Based Didactic Platform for the Learning of Control Engineering

Rafael C. Neto<sup>1</sup>  · Felipe L. A. Trindade<sup>1</sup> · Beatriz R. A. Marques<sup>1</sup> · Gustavo M. S. Azevedo<sup>1</sup> · Eduardo J. Barbosa<sup>1</sup> · Eduardo A. O. Barbosa<sup>1</sup>

Received: 29 March 2022 / Revised: 28 November 2022 / Accepted: 5 December 2022 / Published online: 6 February 2023  
© Brazilian Society for Automatics–SBA 2023

## Abstract

Due to the complexity of the subjects covered in control engineering courses, many students have difficulty in resolving practical control problems. In order to solve this problem, didactic plants can be used as teaching tools to allow students to practice the design of controllers through the investigation of real physical systems. In this sense, this paper proposes an aeropendulum-based didactic platform to be used in control engineering courses. This paper cover all fundamental concepts about aeropendulums, a simulation model built and some suggested practices that can be done using the proposed platform. The experimental results show that the proposed didactic platform is fully functional.

**Keywords** Control engineering · Didactic platform · Aeropendulum · Nonlinear plant

## 1 Introduction

With the technological revolution experienced in recent decades, automatic process control has become fundamental in all areas of engineering and science (Ogata, 2010). In fact, control systems provide an attenuation in the occurrence of human error, increase productivity and restrict waste, leading to better economic results (Smith & Corripio, 2006).

In this scenario, the use of didactic plants as a teaching tool allows students to practice the design of control techniques through the investigation of real physical systems. However, it is important to emphasize that a fundamental part of this investigation is the dynamic modeling of systems, which is also subject in control engineering courses and it is essential for prediction and control purposes (Goodwin & Payne, 1977).

According to (Jasute et al., 2016), most students appreciate practical activities. In fact, they perceive themselves to be more enthusiastic when submitted to significant and non-trivial experiences. Therefore, the use of didactic plants as a pedagogical tool promotes the union between theory and practice, combining the social contribution of the university environment with the development of technical knowledge.

Several companies offer didactic plants to fill this academic gap, examples can be found in (Hamburg, 2022). However, as these tools are usually expensive, the number of institutions that can take advantage of these resources is small. Thus, the production of low-cost didactic plants in universities is a promising solution for the development of technical knowledge.

In this sense, this paper aims to present a low-cost didactic platform based on an aeropendulum. The aeropendulum is a naturally nonlinear system that is relatively simple to control. With this didactic platform, it is possible to practically approach several topics covered in control engineering

Rafael C. Neto, Felipe L. A. Trindade, Beatriz R. A. Marques, Gustavo M. S. Azevedo, Eduardo J. Barbosa and Eduardo A. O. Barbosa have contributed equally to this work.

✉ Rafael C. Neto  
rafael.cavalcantineto@ufpe.br

Felipe L. A. Trindade  
felipe.trindade@ufpe.br

Beatriz R. A. Marques  
beatriz.amos@ufpe.br

Gustavo M. S. Azevedo  
gustavo.msazevedo@ufpe.br

Eduardo J. Barbosa  
eduardo.josebarbosa@ufpe.br

Eduardo A. O. Barbosa  
eduardo.obarbosa@ufpe.br

<sup>1</sup> Department of Electrical Engineering, Universidade Federal de Pernambuco, Avenida da Arquitetura, s/n, Cidade Universitária, Recife, PE 50740-550, Brazil

courses. To validate the operation of the proposed didactic platform, an analog controller implemented with operational amplifiers was used. The main contributions of this paper are:

- Propose a low-cost didactic platform based on an aeropendulum;
- Present all design steps of the proposed platform so that it can be replicated;
- Provide a complete simulation file of the aeropendulum that can also be used in control engineering lessons; and
- Present six control engineering practices that can be done using the proposed platform.

This paper is organized as follows. In Sect. 2, the fundamental principles of an aeropendulum are presented. Section 3 describes the development of the proposed aeropendulum-based didactic platform. In Sect. 4, practices suggestions and experimental results used to validate the proposed didactic platform are presented. Finally, conclusions are presented in Section 5.

## 2 Fundamental Principles of an Aeropendulum

Pendulums are present in many classic engineering problems. A simple pendulum consists of a mass held by a string, which is attached to a support point (Fig. 1a). It is naturally stable since it will always tend to position its mass at the equilibrium point. This equilibrium point is the position where the system is in its lowest energy state (considering no external forces), which, in the case of the pendulum, is the lowest position it can reach.

Although the simple pendulum has great value for the theoretical study of control systems, it cannot be used as a control plant. This happens because the simple pendulum do not have an actuator, what compromises its controllability. However, a good alternative to classical pendulums, but not far from it, is the aeropendulum, which is shown in Fig. 1b.

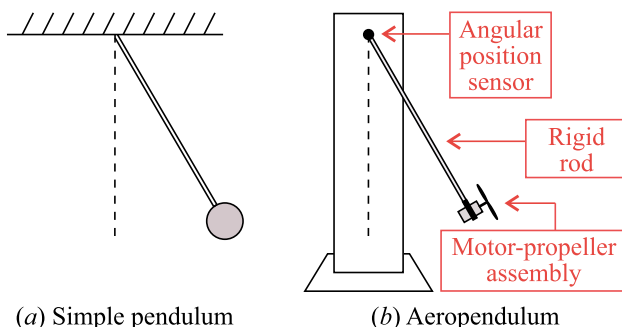


Fig. 1 Examples of pendulum and aeropendulum

It consists of a mechanical pendulum that has a motor with a propeller at its free end (Enikov & Campa, 2012). This motor allows the control system designer to actively control the pendulum position using a feedback loop (Habib et al., 2017).

In order to properly characterize the dynamic behavior of the aeropendulum, it is important to show how it can be mathematically modeled. In this sense, Fig. 2 represents the free-body diagram of the forces acting on this system. Using this diagram and applying Newton's second law for rotation, it can be seen that:

$$(F - m_{\text{motor}} g \sin(\theta))L - m_{\text{rod}} g \sin(\theta) \frac{L}{2} - \mu\omega = J\alpha, \quad (1)$$

in which  $m_{\text{motor}}$  corresponds to the mass of the motor-propeller assembly,  $m_{\text{rod}}$  is the mass of the rod,  $L$  refers to the length of the rod,  $J$  is the moment of inertia of the aeropendulum,  $\alpha$  refers to the angular acceleration,  $g$  is the gravity and  $\mu\omega$  represents the friction torque.

In this system, it is desired to apply a thrust force  $\mathbf{F}$  to control the aeropendulum's angular position  $\theta$ . Thus, rearranging (1), it can be rewritten so that one can obtain the following differential equation:

$$J\ddot{\theta} + \mu\dot{\theta} + \sin(\theta)Lg \left( m_{\text{motor}} + \frac{m_{\text{rod}}}{2} \right) - FL = 0, \quad (2)$$

It is important to note that the output variable of the system represented in (2) shows itself as an argument of a sine function. This characteristic indicates that this is a nonlinear system. In addition, it is also important to note that the thrust force is applied by the motor-propeller assembly, therefore depending on the motor voltage supply. In this way, the motor voltage supply can be considered the system input.

The mechanical structure of an aeropendulum usually has a significantly slower dynamic behavior than the propeller-

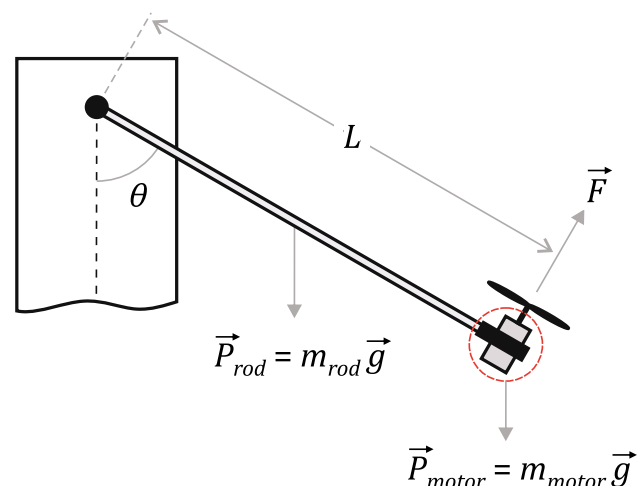


Fig. 2 Free-body diagram of an aeropendulum

motor assembly. Thus, the mechanical structure of the aeropendulum has dominant dynamic characteristics in this system. In this sense, the dynamic model of the system can be simplified by considering the voltage-thrust relation as having a zero-order behavior ( $F(V)$ ). By doing this, (2) can be rewritten as:

$$J\ddot{\theta} + \mu\dot{\theta} + \sin(\theta)Lg\left(m_{\text{motor}} + \frac{m_{\text{rod}}}{2}\right) - F(V)L = 0. \quad (3)$$

By modeling the motor as a zero-order system, it becomes possible to evaluate the motor operating ranges (deadband, linear operation and saturation) and the voltage-thrust gain for each of these ranges, which is useful to understand the system. As shown in Sect. 4, this simplification results in a good model approximation; however, if one desires to represent the complete dynamics of the motor in his/her model, one can consider the equations and the parameters estimation presented in (Karnavas and Chasiotis, 2016).

The moment of inertia of the aeropendulum can be calculated considering the motor-propeller assembly as a sphere of uniform mass. By doing so, the aeropendulum can be simplified into a simple pendulum, as shown in Fig. 1a. Thus, from the use of the parallel axis theorem (Halliday et al., 2018), the moment of inertia of the aeropendulum is given by

$$J = \frac{m_{\text{rod}}L^2}{3} + \left[ \frac{2m_{\text{motor}}r^2}{5} + m_{\text{motor}}(L+r)^2 \right], \quad (4)$$

where  $r$  is the radius of the sphere that represents the motor-propeller assembly.

In addition to being relatively simple to control, the aeropendulum brings up several topics that are covered in engineering graduation courses, what makes the proposed didactic platform very user friendly. Topics such as mechanical physics, system modeling, system identification, control techniques and design of signal conditioning circuits can be approached using an aeropendulum-based didactic platform. As a matter of fact, pendulums are classic systems control problems, so they are quite familiar to engineering undergraduate students.

### 3 The Aeropendulum-Based Didactic Platform

The aeropendulum-based didactic platform consists of a mechanical structure of an aeropendulum together with its electronic structure, which aggregates the necessary circuits for the proper functioning of the didactic platform. The 3D model of the proposed didactic platform is shown in Fig. 3.

As shown in Fig. 3, the aeropendulum has several components. The primary objectives of each part of the system are:

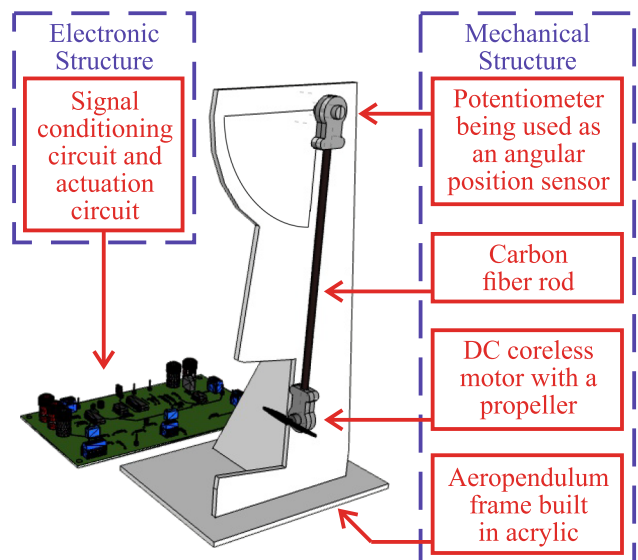


**Fig. 3** Three-dimensional model of the aeropendulum-based didactic platform

- Mechanical Structure:** It was designed to be the aeropendulum frame together with its actuator and its angular position sensor. As it is the mechanical part of a teaching kit, it must be portable and small, so as to allow comfortable use on a workbench. Besides, it also should present a pleasant design to students, it must be built with durable materials and its components must be easy to replace;
- Electronic Structure:** It was designed to work as interface between the mechanical structure of the aeropendulum and the controller (not included in the didactic platform). It contains a signal processing circuit designed to measure the aeropendulum's angular position and an actuation circuit, which works as electrical drive for the aeropendulum's motor. These circuits were designed in a way that students can use either digital or analog controllers.

In addition to the physical parts of the aeropendulum described above, an simulation file was also developed for MATLAB/Simulink and Scilab/Xcos softwares. The main objective of these files is to provide the control engineering teacher some tools that can help him to explain the didactic platform to the students. It is important to emphasize that the didactic platform is not controlled by any of these softwares. As a matter of fact, the didactic platform requires the use of an analog or digital controller that must be developed by the students.

Since it is designed to be a didactic platform, the aeropendulum should meet some requirements to ensure its proper functioning, usability and security. The main desired requirements of the platform are:

- Voltage and current demanded by the didactic platform must be supported by a commercial regulated power supply;
- The printed circuit board (PCB) must have clear indications of input, output and supported voltages;
- The signal conditioning circuit must be printed on the top silkscreen layer of the PCB in order to facilitate its understanding;
- The didactic platform must have a low-cost in order to make it viable.

### 3.1 Mechanical Structure

The mechanical structure of the proposed didactic platform consists of five parts: (i) an aeropendulum frame; (ii) a rod; (iii) a motor-propeller assembly; (iv) a potentiometer; and (v) connectors that couple the potentiometer and the motor on the rod. These parts are briefly described below. The complete aeropendulum is shown in Fig. 4a.

#### 3.1.1 Aeropendulum Frame and Rod

The aeropendulum frame is a mechanical frame on which the rotation axis of the aeropendulum is mounted. This frame is composed by three smaller parts: the base frame; the front frame; and rear bracket. This structure is shown in Fig. 4b.

The choice of material to be used for the building the aeropendulum frame took into account points such as the material's weight, price, finishing quality and ease of machining. Based on these criteria, the aeropendulum frame was built using an acrylic sheet with thickness of 4mm. The acrylic sheet was cut using a 3-axis CNC cutting machine with a 2-mm ball nose end mill. The files for manufacturing the parts are available at: <https://github.com/rafaelcneto/Aeropendulum>.

Regarding the aeropendulum's rod, it is observed that the choice of its material has the following restrictions:

- **It must have low weight:** Ideally, the aeropendulum's rod should be massless. As a matter of fact, the rod cannot be so heavy that the motor-propeller assembly cannot generate the necessary thrust to increase the aeropendulum angulation.
- **It must have high rigidity:** It cannot be flexible.

Because of such factors, a 5-mm carbon fiber (25cm long) rod was used in this didactic platform.

#### 3.1.2 The Motor-Propeller Assembly and the Potentiometer

A DC coreless motor was used in this aeropendulum, given that it operates with high rotation speeds and can be powered using a DC voltage source. This second characteristic is very

important to a didactic platform since DC voltage sources are commonly used in engineering courses.

The DC coreless motor can be controlled using pulse-width modulation (PWM) techniques and a simple switching circuit, avoiding the use of complex electronic speed controllers such as those used for AC brushless motors. Since there is no iron core in this motor, it is characterized for having a small size and a light weight, which makes the motor-propeller assembly also small and compact. As consequence, it has a lower moment of inertia, which contributes to faster acceleration and deceleration than regular DC motors (Collins, 2018). Besides that, the DC coreless motor also has a high power for its size, being able to provide a good amount of thrust when coupled with a propeller on its shaft.

The reference of the DC coreless motor used in the prototype is: 1S 1020 3.7V. This means that its nominal voltage is 3.7V; it is normally power supplied using a single cell battery (1S); and its size is 10mmx20mm (1020). The propeller used in the prototype is a quadcopter propeller with diameter of 76.3mm. The motor-propeller assembly is shown in Fig. 4c.

Regarding the potentiometer, it must be accurate and linear. The demand for high accuracy is due to the fact that, since it is used as an angular position sensor, any incorrect measurement of its resistance can negatively impact the performance and the stability of the control system. Also, it is important for the potentiometer to be linear so that the angular position sensor can have a linear measuring range. Based on these requirements, a precision multi-turn potentiometer is used in the prototype (Fig. 4d).

Connectors built using an acrylic sheet with thickness of 4 mm were used to couple the potentiometer and the DC coreless motor on the aeropendulum's rod. Both connectors are composed of two symmetrical parts that press on the aeropendulum's rod, making the assembly rigid. These parts are fixed using screws and nuts, as shown in Fig. 4c and e. The files for manufacturing the parts are available at: <https://github.com/rafaelcneto/Aeropendulum>.

### 3.2 Electronic Structure

As shown in Fig. 3, the electronic structure of the aeropendulum-based didactic platform consists of two electronic circuits: a signal conditioning circuit; and an actuation circuit. These circuits are briefly described in this subsection.

#### 3.2.1 Signal Conditioning Circuit

As described before, the proposed didactic platform demands a signal conditioning circuit to convert the potentiometer resistance measurement, which is used to measure the aeropendulum's angular position, into a voltage measure. The desired output voltage range for this circuit is from 0V to 3.3V, as it can be used for both analog and digital control

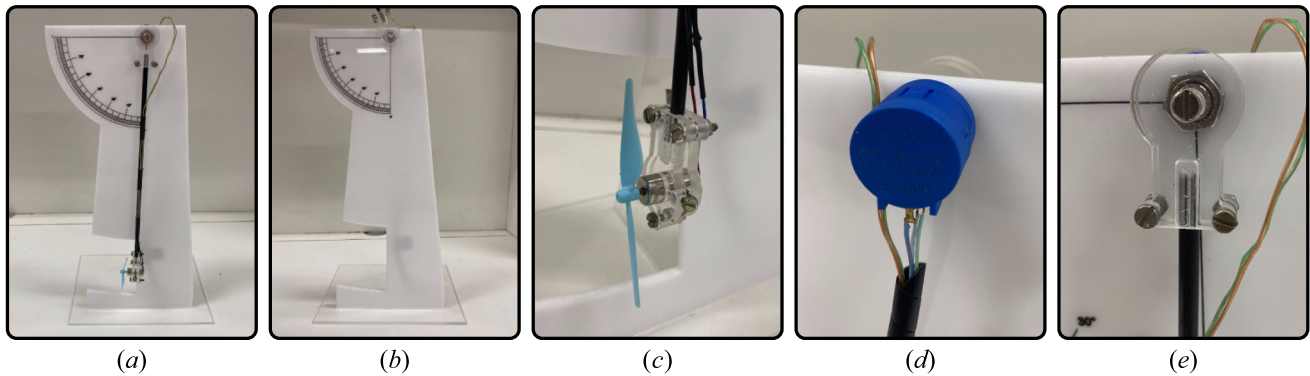


**Fig. 4** Mechanical structure of the aeropendulum: **a** complete aeropendulum; **b** aeropendulum frame; **c** motor-propeller assembly with the connector to couple it on the aeropendulum's rod; **d** multi-turn potentiometer; and **e** connector used to couple the potentiometer on the aeropendulum's rod

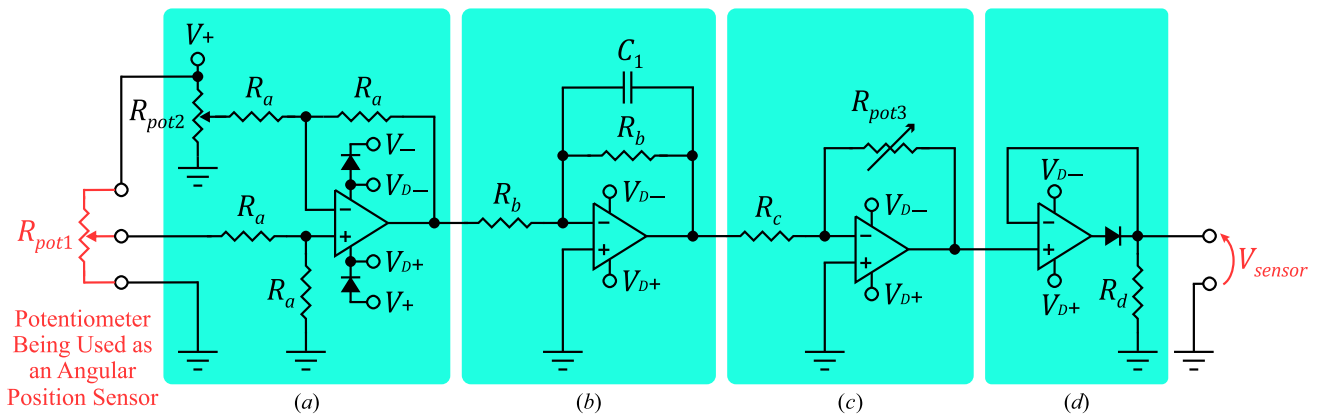


**Fig. 5** Signal conditioning circuit. This circuit is composed by four stages: **a** an offset removal stage; **b** an anti-aliasing filter; **c** a gain correction stage; and **d** a protection stage

practices (most microcontrollers can measure voltages in this range through their ADC ports). Thus, the design requirements for this circuit are:

- (i) It must have an offset removal stage and a gain correction stage, which will provide the output voltage range adjustment;
- (ii) It must have an anti-aliasing filter for digital control purposes; and
- (iii) It must have a protection stage to prevent negative voltages from reaching the output of the signal conditioning circuit.

The complete circuit diagram is shown in Fig. 5. The values used for the components are shown in Table 1. All four stages of this circuit are briefly described below.

In order to calibrate the signal conditioning circuit, it is first necessary to understand how its signal is captured. In this didactic platform, the potentiometer's axis of  $R_{pot1}$  is directly connected to the aeropendulum rod (Fig. 3). Thus, any change in the angulation of the aeropendulum's rod will

also change the potentiometer resistance and, therefore, its voltage.

Since it is intended to use an output range from  $0^\circ$  to  $90^\circ$  for the angular position of the aeropendulum's rod, the output voltage of the signal conditioning circuit ( $V_{sensor}$ ) must be 0V when the angular position is  $0^\circ$  and 3.3V when the angular position is  $90^\circ$ . Any other output voltage will obey a linear scale in this interval. Then, in order to calibrate the signal conditioning circuit, one must do the following steps:

1. **In the offset removal stage** (Fig. 5a): Firstly, the aeropendulum rod must be positioned in its start position ( $0^\circ$ ). Then, the trimmer potentiometer  $R_{pot2}$  must be adjusted so that the output voltage of the circuit becomes 0V, i.e.,

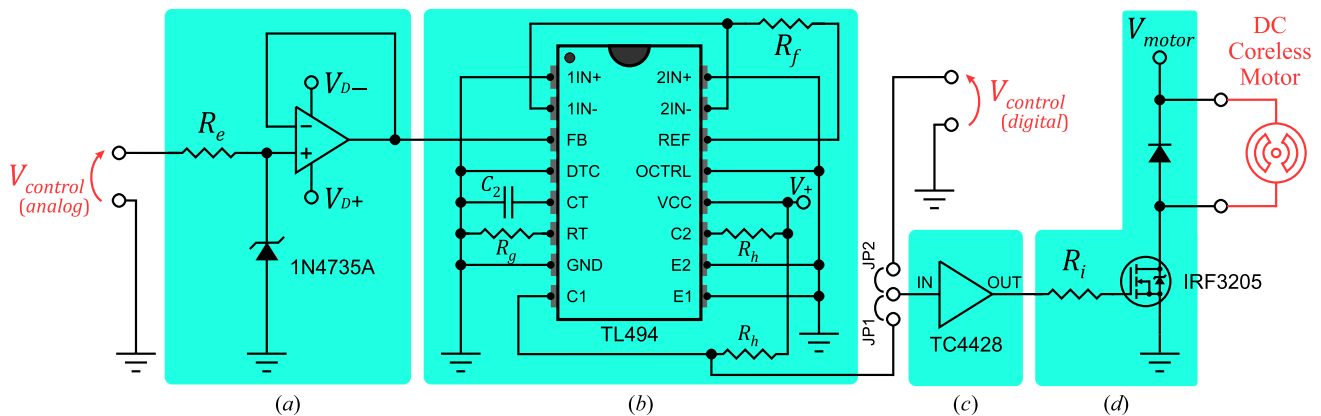
$$V_{sensor}(0^\circ) = 0V. \quad (5)$$

This step will calibrate the lower threshold of the output voltage range; and



**Table 1** Values used for the components of the circuits presented in Fig. 5 and 6

$R_a$	$R_b$	$R_c$	$R_d$	$R_e$	$R_f$	$R_g$	$R_h$	$R_i$	$C_1$	$C_2$	$R_{pot1}$	$R_{pot2}$	$R_{pot3}$	$V_+$	$V_-$	$V_{motor}$
1M $\Omega$	10k $\Omega$	1k $\Omega$	10k $\Omega$	10k $\Omega$	50k $\Omega$	10k $\Omega$	1k $\Omega$	100 $\Omega$	2.2nF	10nF	1k $\Omega$	1k $\Omega$	10k $\Omega$	+12V	−12V	3.5V

**Fig. 6** Actuation circuit. This circuit is composed by four stages: **a** a voltage limiter stage; **b** a PWM generation circuit for analog control practices; **c** a MOSFET driver; and **d** a DC motor speed control circuit.

2. **In the gain correction stage** (Fig. 5c): Since  $V_{\text{sensor}}(0^\circ)$  is calibrated to be 0V, the upper threshold ( $V_{\text{sensor}}(90^\circ)$ ) can be selected using the gain correction stage. Thus, in order to calibrate  $V_{\text{sensor}}(90^\circ)$ , one must hold the aeropendulum rod in its upper threshold position ( $90^\circ$ ). Then, the trimmer potentiometer  $R_{\text{pot}3}$  must be adjusted so that the output voltage of circuit becomes 3.3V, i.e.,

$$V_{\text{sensor}}(90^\circ) = 3.3V. \quad (6)$$

It should be noted that the input impedance of the signal conditioning circuit must be high so that the potentiometer resistance measurement of  $R_{\text{pot}1}$  is not compromised. Alternatively, an operational amplifier (OpAmp) can be used as buffer to guarantee this characteristic.

The anti-aliasing filter, shown in Fig. 5b, is an unity-gain low-pass filter frequently used in digital control practices. It is used to ensure that the input signal sampling is not harmed by the aliasing effect. Thus, following the Nyquist theorem (Kuo, 1995), this filter is designed to have cut-off frequency around half of the sampling frequency. Then, based on a microcontroller with an ADC sampling frequency of 16kHz, the cut-off frequency of the anti-aliasing filter should be around 8kHz.

Finally, a protection stage must be used to ensure that negative voltage values cannot occur at the output of the signal conditioning circuit. Therefore, an OpAmp was used in a superdiode configuration, which, in addition to not allowing negative output voltage values, it does not have the knee

circuit. This circuit has a jumper connector to select whether an analog controller or a digital controller will be applied

voltage drop of a regular diode, which is usually around 0.7V for silicon diodes.

### 3.2.2 Actuation Circuit

The actuation circuit is responsible for driving the DC coreless motor and for controlling its average supply voltage using the control action (here referred as  $V_{\text{control}}$ ). In this circuit, the DC motor speed must be controlled by modulating the motor supply voltage using a PWM strategy. Therefore, the design requirements for this circuit are:

- It must have a PWM control circuit, which will generate the PWM using the control action  $V_{\text{control}}$  for analog controllers;
- It must have a protection stage to prevent negative voltages and overvoltages from reaching the PWM control circuit (for analog control action); and
- It must have a DC motor speed control circuit that should use a PWM signal as input signal.

The complete circuit diagram is shown in Fig. 6. The values used for the components are shown in Table 1. All four stages of this circuit are briefly described below.

Regarding the DC motor speed control circuit, since the aeropendulum was planned to operate with angular position between  $0^\circ$  and  $90^\circ$ , which means the DC motor must only rotate in one direction, a DC dimmer circuit using a low-side MOSFET can be used for this purpose (Fig. 6d). A freewheel-

ing diode was added to this stage to prevent the MOSFET from being damaged by flyback voltages caused by the DC motor (as it behaves as an inductive load).

In order to control the MOSFET switching, it is necessary to generate a PWM signal in its gate pin. As shown in Fig. 6, this PWM signal can be generated by a microcontroller or a DSP (using  $V_{control}^{control(digital)}$  as input signal), for digital control practices, or by a TL494 integrated circuit (using  $V_{control}^{control(analog)}$  as input signal), for analog control practices. The TL494 integrated circuit (IC) is a fixed frequency, PWM control circuit designed primarily for switch mode power supply control. It should be noted that jumpers JP1 and JP2 are used to select whether the circuit input signal will be  $V_{control}^{control(analog)}$  or  $V_{control}^{control(digital)}$ . In addition, a MOSFET driver (Fig. 6c) is necessary to convert the low-power PWM signal to a high-current input for the gate of the MOSFET.

In case one chooses to perform analog control practices using the proposed didactic platform, it is important to limit the analog control action  $V_{control}^{control(analog)}$  to avoid damage the TL494 IC. In the proposed platform, this feature is implemented using a voltage limiter stage composed by a clipping circuit (based on a Zener diode) and by a voltage buffer, as shown in Fig. 6a.

Since this paper aims to propose a didactic platform, its PCB must be didactic and intuitive. In this sense, the following design guidelines were followed:

1. The input voltage and output voltage ranges are indicated in the PCB silkscreen layer;
2. The input and output terminals are identified in the PCB silkscreen layer;
3. Banana sockets are used to simplify the power supply connections of the PCB;
4. Pin headers are used to provide easy access point to measure  $V_{control}$ ,  $V_{sensor}$  and the MOSFET gate signals; and
5. The signal conditioning circuit is drawn in the PCB silkscreen layer.

The 3D model of the designed PCB is shown in Fig. 7. Its Gerber and design files can be downloaded using the following link: <https://github.com/rafaelcneto/Aeropendulum>.

### 3.3 Simulation Files for Teaching Support

Based on the dynamic modeling presented in Sect. 2, simulation files of an aeropendulum were developed for MATLAB/Simulink and Scilab/Scos softwares. These files are available at: <https://github.com/rafaelcneto/Aeropendulum>. They work as support tools for the control engineering teacher as they allow students to evaluate the control characteristics of the system, such as settling time, steady-state error and maximum percentage overshoot, before controlling

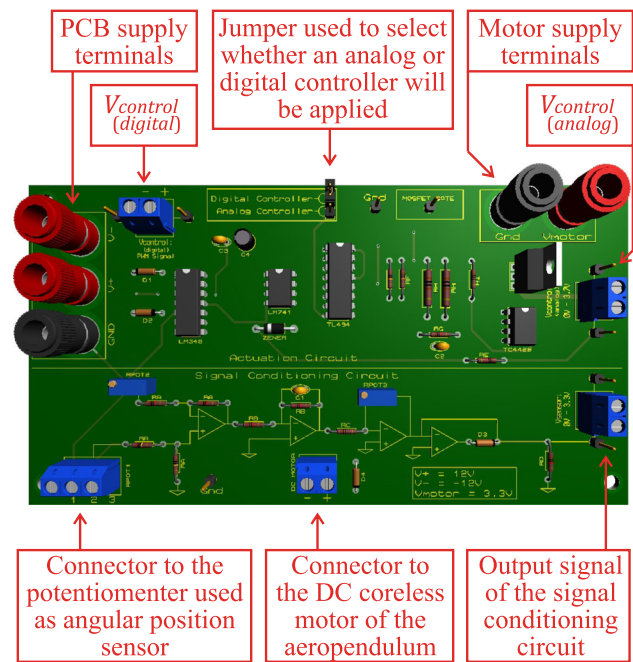


**Fig. 7** Three-dimensional model of the designed PCB. This board contains both signal conditioning circuit and actuation circuit

the real plant. The MATLAB/Simulink version includes a 3D model simulation of the aeropendulum.

The block diagram of the dynamic model of the aeropendulum is shown in Fig. 8. As shown in Fig. 8, the dynamic model of the aeropendulum has the following parameters: the voltage-thrust relation ( $F(V)$ ); the friction coefficient used to model the impact of the resistance imposed by the potentiometer on the aeropendulum's axis variation ( $\mu$ ); gravity ( $g$ ); the mass of the rod ( $m_{rod}$ ); the mass of the motor-propeller assembly ( $m_{motor}$ ); the length of the rod ( $L$ ); and the moment of inertia of the aeropendulum ( $J$ ). The parameters  $m_{rod}$ ,  $m_{motor}$  and  $L$  can be easily measured since the aeropendulum was already built, while the parameter  $J$  can be calculated using (4). On the other hand, the parameters  $F(V)$  and  $\mu$  can be obtained experimentally, as discussed in Sect. 4.

The simulation files are available to enable control engineering teachers to show their undergraduate students how to design a closed-loop control system. In this context, the students would carry out: (i) the design of the controller to be used; (ii) the simulation of the closed-loop control system in MATLAB/Simulink or Scilab/Xcos; and, finally, (iii) the practical implementation of the controller using the physical didactic platform.

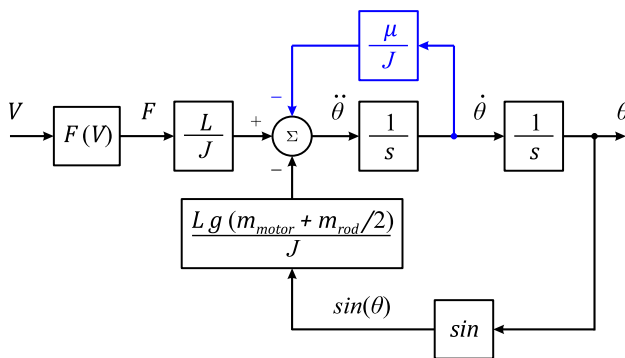


**Fig. 8** Block diagram of the dynamic model of the aeropendulum. The impact of the resistance imposed by the potentiometer on the aeropendulum's axis variation is modeled in blue

In this scenario, the control engineering teachers has two most common ways of working:

- **If the teachers plans to work with analog control:** During step (ii), the student can implement the controller either using its transfer function in Laplace domain or using a circuit based on OpAmps. As consequence, students would be able to migrate to a practical implementation (step (iii)) using an analog controller without major difficulties.
- **If the teachers plans to work with digital control:** During step (ii), the student can implement the controller either using its transfer function in z-domain or using its line-code implementation through a structured programming block. As consequence, students would be able to migrate to practical implementation (step (iii)) using a digital controller without major difficulties.

It is important to highlight that the control engineering teacher can lead the teaching process without using the simulation files available here. These files are only available to assist the teacher, they do not replace either the physical didactic platform or the controller.

### 3.4 Cost Analysis

The costs to build the proposed didactic platform were accounted for evaluating its viability. In fact, these costs can be divided into two parts: costs associated with the mechanical structure of the project (Table 2); and costs associated with the electronic part of the project (Table 3). The costs associated with acrylic cutting were not taken into account as these cuts were performed using a CNC milling machine available at the educational institution's facilities.

As can be concluded from Table 2 and 3, it takes around US\$ 46.17 to build the proposed didactic platform (without taking the CNC milling process cost into account). This value

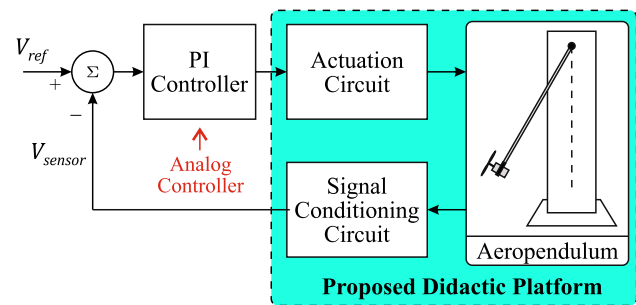


**Fig. 9** Block diagram of the complete control system

is considerably lower than the acquisition costs of didactic plants sold by companies in this field.

## 4 Experimental Validation of the Didactic Platform

In order to experimentally validate the proposed didactic platform, an analog controller was used to control the aeropendulum's angular position. The analog controller was built using OpAmps to work as a proportional-integral (PI) controller (Ogata, 2010). The block diagram of the complete control system is shown in Fig. 9. The subtractor was implemented using a circuit with OpAmp and the reference voltage ( $V_{ref}$ ) was provided by a DC voltage source. Figure 10 shows a picture of the experimental setup.

As the output voltage of the signal conditioning circuit ( $V_{sensor}$ ) is always between 0V and 3.3V (which is used to represent the angular position range), the reference signal of the control system ( $V_{ref}$ ) should also be a voltage in this operating range. Besides that, since the reference signal of this system is usually a constant value, then, based on the internal model principle (Francis & Wonham, 1975), a PI controller is enough to guarantee zero steady-state error (given that the system is stable). For the evaluation presented in this paper, the proportional and integral gains are  $K_p = 0.095$  and  $K_i = 0.95$ , respectively.

Figure 11 presents the results obtained for the experimental setup represented by the diagram shown in Fig. 9. These results were obtained applying a 2V constant signal as reference of the evaluated control system. It should be noted that this is equivalent to apply  $2V \cdot \frac{90^\circ - 0^\circ}{(3.3V - 0V)} \approx 54, 5^\circ$  as reference signal if the voltage-angular position conversions are disregard. As it can be seen, the PI controller leads to a zero steady-state error.

After a first inspection on the results shown in Fig. 11, one can prematurely conclude that the closed-loop system has a transport delay. As a matter of fact, this characteristic occurs due to the fact that the steady-state voltage-thrust relation of the motor-propeller assembly is nonlinear, as shown in



**Table 2** Costs associated with the mechanical structure of the proposed didactic platform

Item	Unit price	Qty	Ext price
4mm acrylic sheet*	US\$ 60/ $m^2$	0.12 $m^2$	US\$ 7.20
Screws and nuts for potentiometer and DC motor holders*	US\$ 0.12	6	US\$ 0.72
Carbon fiber rod (diameter of 5mm)**	US\$ 4.20/ $m$	0.25 $m$	US\$ 1.05
DC coreless motor (1S 1020 3.7V) with propeller**	US\$ 1.85	1	US\$ 1.85
Potentiometer***	US\$ 13.16	1	US\$ 13.16
Total	—	—	US\$ 23.98

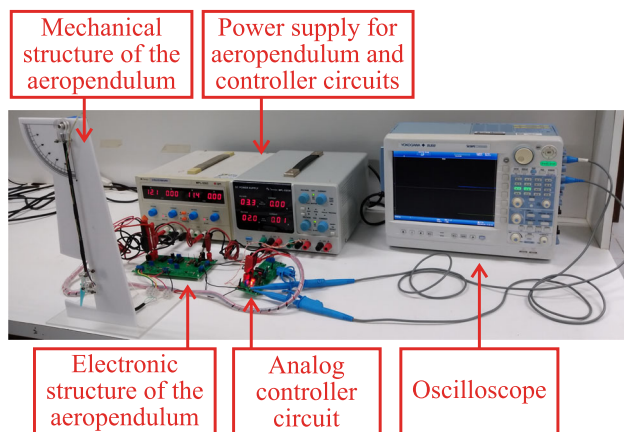
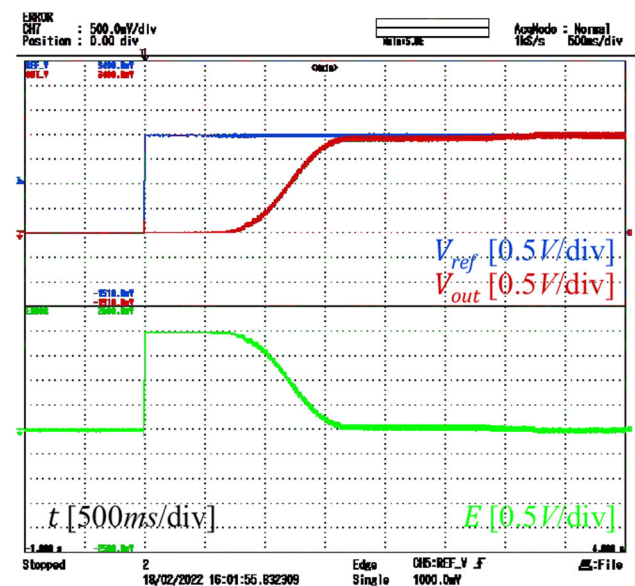
\* Purchased from local suppliers

\*\* Purchased from <https://www.aliexpress.com>\*\*\* Purchased from <https://www.digikey.com>**Table 3** Costs associated with the electronic structure of the proposed didactic platform

Item	Price
Resistors*	US\$ 0.70
Capacitors*	US\$ 0.69
Integrated circuits (TL494, TC4428, LM348 and LM741)*	US\$ 4.26
MOSFET (IRF3205)*	US\$ 1.63
Trimmer potentiometers*	US\$ 3.33
Diodes*	US\$ 0.88
Sockets, banana jacks and connectors**	US\$ 6.76
PCB manufacturing process*** (price per board)	US\$ 3.94
Total	US\$ 22.19

\* Purchased from <https://www.digikey.com>

\*\* Purchased from local suppliers

\*\*\* Purchased from [https://www.seeedstudio.com/fusion\\_pcb.html](https://www.seeedstudio.com/fusion_pcb.html)**Fig. 10** Experimental setup used to validate the proposed didactic platform**Fig. 11** Experimental results obtained using the system shown in Fig. 9. Top plot: reference voltage signal in blue and output voltage of the signal conditioning circuit in red. Bottom plot: error voltage signal in green (Color figure online)

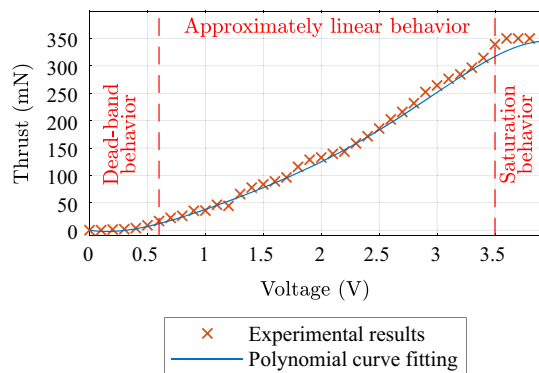


**Fig. 12** Voltage-thrust relation of the motor-propeller assembly (obtained experimentally)

Fig. 12 (obtained experimentally). The voltage-thrust relation shown in Fig. 12 can be divided into three distinct operating ranges:

- (i) The range between 0V and 0.6V, whose voltage-thrust relation can be approximated by a dead-band behavior;
- (ii) The range between 0.6V and 3.5V, whose voltage-thrust relation can be approximated by a linear behavior; and
- (iii) The range between 3.5V and 3.7V, whose voltage-thrust relation can be approximated by a saturation behavior.

After enabling the control system, the PI controller begins to generate the control action. One should note that the dynamic behavior of the motor-propeller assembly, which was disregarded until now, begins to impact the control system.

In case one opts for simplifying the dynamic behavior of the motor-propeller assembly into a zero-order system based in the steady-state curve shown in Fig. 12, it should be noted that its initial error would be 2V, which would imply an initial control action of 0.19V (only provided by the proportional action). According to Fig. 12, if this voltage is applied to the motor terminals, it would still operate in its dead-band, which would not cause any change in the aeropendulum's angular position. However, as time passes, the integral action increases. In fact, the integral action increases to the point that the control action becomes large enough to allow the motor-propeller assembly to operate in its linear region, making the aeropendulum's angular position to change. As discussed in Sect. 2, the simplification described above is possible because the motor electromagnetic dynamics is significantly faster than the mechanical motion of the aeropendulum, thus, the motor electromagnetic dynamic response can be ignored.

The curve that represents the zero-order system described in the previous paragraph is used in the simulation files built in MATLAB/Simulink and Scilab/Xcos softwares as the voltage-thrust relation  $F(V)$  (described in Sect. 3). As  $\mu$  is

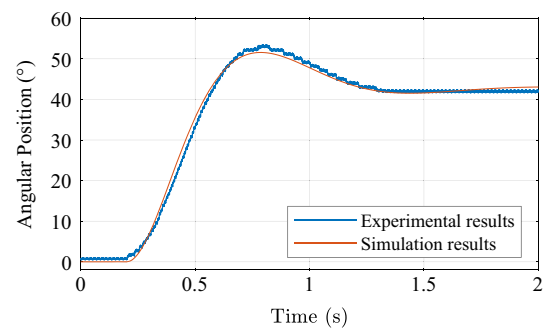


**Fig. 13** Open-loop step responses of the simulated and physical didactic plants

the only parameter that has not yet been obtained, one must obtain the open-loop step response of the physical didactic plant for estimating it. With this response in hands, the parameter  $\mu$  can be manually tuned in the simulation files until the open-loop step response of the simulated didactic plant matches the open-loop step response of the physical plant (Fig. 13). Differences may exist in the responses due to unconsidered dynamics, such as the DC motor dynamics. The parameters used in this simulation are presented in Table 4.

It can be noted that the discussion presented so far in this section shows that not only the didactic platform works, but it can also be used to give an experimental perspective about some control engineering issues, such as system characterization, nonlinear systems, control system design and dynamic modeling. In this context, some practices that can be done using the proposed didactic platform are suggested below.

#### 4.1 Suggested Practices

The key issues that can be worked with students by using the proposed didactic platform are:

- System identification strategies;
- Design and experimental validation of classical controllers using heuristic and non-heuristic approaches;
- Experimental comparison of type 0 and type 1 control systems;
- Experimental comparison of underdamped and overdamped responses; and
- Experimental evaluation of the behavior of nonlinear systems.

Based on the issues presented above, six distinct control engineering practices are suggested below.

1. **Practice 1:** A gray-box model is a hybrid model that combines white-box and black-box modeling approaches. A conventional gray-box models the evaluated sys-

**Table 4** Parameters used for simulation of the aeropendulum.  $V$  is the input signal of the system, as indicated in Fig. 8

Parameters					$F(V) = A \cdot V^3 + B \cdot V^2 + C \cdot V + D$			
$L$	$m_{\text{motor}}$	$m_{\text{rod}}$	$J$	$\mu$	$A$	$B$	$C$	$D$
0.2850 m	0.0166 kg	0.0070 kg	0.0013 kg.m <sup>2</sup>	0.0074	− 0.0038	0.0391	0.0031	0

tem using a physical formulation in order to keep its physical interpretation; however, experimental data are used to estimate the system's parameters (Bohlin, 2006). As presented before, the simulations built for MATLAB/Simulink and Scilab/Xcos are based in a gray-box modeling approach. Thus, the control engineering teacher can ask students to develop this same model in a new simulation file and compare its response with the one obtained for the physical didactic platform. By doing this, students have a better understanding of how and when they should use black-box, white-box, and gray-box modeling strategies.

2. **Practice 2:** Once the mathematical model that represent the aeropendulum is obtained, it can be used to design a classical controller. In this scenario, the control engineering teacher can ask students to design the controller using a non-heuristic methods, such as pole-zero cancellation or control design based in root locus tool, to meet some project requirements. Students could experimentally the controller.
3. **Practice 3:** Considering that the students do not know the mathematical model that represents the dynamics of the aeropendulum, the control engineering teacher can ask them to design the controller using a heuristic PID tuning method, such as Ziegler-Nichols step response method (Åström and Häggnd, 2004). By doing so, they would see the experimental limitations of such approach.
4. **Practice 4:** In order to present how controllers based on the internal model principle (Francis & Wonham, 1976) can be used to obtain zero steady-state error (for instance, the integral controller for step inputs), the control engineering teacher can ask students to compare the steady-state responses of the aeropendulum when it is controlled by a proportional controller and by a proportional-integral controller. This can be done to understand the differences between type 0 and type 1 control systems.
5. **Practice 5:** Once the mathematical model that can represent the aeropendulum is obtained, the control engineering teacher can ask students to design the controller so that the systems' response becomes underdamped or overdamped. Thus, students would experimentally compare the system response for underdamped and overdamped configurations.

6. **Practice 6:** Since the aeropendulum is a nonlinear system, it can be used to experimentally approach the characteristics of nonlinear systems. Besides that, it also can be used to show students how to experimentally implement linearization techniques.

These practices were performed by undergraduate students of the Control and Automation Engineering Course of Universidade Federal de Pernambuco (Brazil) for two semesters. All students gave positive feedback regarding the use of this didactic platform in classroom.

## 5 Conclusion

This paper proposes an aeropendulum-based didactic platform that can be used by control engineering teachers in practical lessons. In order to do so, the main concepts about an aeropendulum, about its mechanical and electronic structures and about how to simulate it are presented. Since the cost to build the proposed didactic platform is significantly lower than the acquisition cost of commercial didactic plants, it proves to be a good alternative for education institutions.

The experimental results presented in this paper show that the proposed didactic platform is fully functional. Besides that, it is important to point that all suggested practices were already applied to undergraduate students, who indicated that the proposed platform has positively impacted their technical formation.

## Declarations

**Conflict of interest** The authors declare that there is no conflict of interest regarding the publication of this paper.

## References

- Astrom, K., & Hagnd, T. (2004). Revisiting the ziegler-nichols step response method for pid control. *Journal of Process Control*, 14(6), 635–650.
- Bohlin, T. (2006). *Practical grey-box process identification: Theory and applications*. London: Springer.
- Collins, D. (2018). What are coreless DC motors? Available: <https://www.motioncontroltips.com/what-are-coreless-dc-motors/>.
- Enikov, E. T., & Campa, G. (2012). Mechatronic aeropendulum: Demonstration of linear and nonlinear feedback control principles with matlab/simulink real-time windows target. *IEEE Transactions on Education*, 55(4), 538–545.

- Francis, B. A., & Wonham, W. M. (1975). The internal model principle for linear multivariable regulators. *Applied Mathematics and Optimization*, 2(2), 170–194.
- Francis, B., & Wonham, W. (1976). The internal model principle of control theory. *Automatica*, 12(5), 457–465.
- Goodwin, G., & Payne, R. (1977). *Dynamic system identification: Experiment design and data analysis*. Cambridge: Academic Press.
- Habib, G., Miklos, A., Enikov, E. T., Stepan, G., & Rega, G. (2017). Nonlinear model-based parameter estimation and stability analysis of an aero-pendulum subject to digital delayed control. *International Journal of Dynamics and Control*, 5, 629–643.
- Halliday, D., Resnick, R., & Walker, J. (2018). *Fundamentals of physics*. New York: Wiley.
- Hamburg, G. (2020). Hands-on teaching engineering. [Online]. Available: [https://www.gunt.de/images/download/Cat\\_Teaching\\_Engineering\\_neutral\\_english.pdf](https://www.gunt.de/images/download/Cat_Teaching_Engineering_neutral_english.pdf)
- Jasute, E., Kubilinskiene, S., Juskeviciene, A., & Kurilovas, E. (2016). Personalised learning methods and activities for computer engineering education\*. *International Journal of Engineering Education*, 32(01), 1078–1086.
- Karnavas Y. L. and Chasiotis I. D. (2016) Pmdc coreless micro-motor parameters estimation through grey wolf optimizer. In 2016 XXII International conference on electrical machines (ICEM),UK pp. 865–870.
- Kuo, B. (1995). *Digital control systems*. Oxford: Oxford University Press.
- Ogata, K. (2010). *Modern control engineering*. New York: Prentice Hall.
- Smith, C., & Corripio, A. (2006). *Principles and practices of automatic process control*. New York: Wiley.

**Publisher's Note** Springer Nature remains neutral with regard to jurisdictional claims in published maps and institutional affiliations.

Springer Nature or its licensor (e.g. a society or other partner) holds exclusive rights to this article under a publishing agreement with the author(s) or other rightsholder(s); author self-archiving of the accepted manuscript version of this article is solely governed by the terms of such publishing agreement and applicable law.